

An improved quasar detection method in EROS-2 and MACHO LMC datasets

K. Pichara,^{1,3} P. Protopapas,^{2,3} D.-W. Kim,^{2,3} J.-B. Marquette,⁴ and P. Tisserand⁵

¹Computer Science Department, Pontificia Universidad Católica de Chile, Santiago, Chile.

²Harvard-Smithsonian Center for Astrophysics, Cambridge, MA, USA

³Institute for Applied Computational Science, Harvard University, Cambridge, MA, USA

⁴UPMC-CNRS, UMR7095, Institut d'Astrophysique de Paris, F-75014, Paris, France

⁵Research School of Astronomy and Astrophysics, Australian National University, Canberra, Australia

ABSTRACT

We present a new classification method for quasar identification in the EROS-2 and MACHO datasets based on a boosted version of Random Forest classifier. We use a set of variability features including parameters of a continuous auto regressive model. We prove that continuous auto regressive parameters are very important discriminators in the classification process. We create two training sets (one for EROS-2 and one for MACHO datasets) using known quasars found in the LMC. Our model's accuracy in both EROS-2 and MACHO training sets is about 90% precision and 86% recall, improving the state of the art models accuracy in quasar detection. We apply the model on the complete, including 28 million objects, EROS-2 and MACHO LMC datasets, finding 1160 and 2551 candidates respectively. To further validate our list of candidates, we crossmatched our list with a previous 663 known strong candidates, getting 74% of matches for MACHO and 40% in EROS. The main difference on matching level is because EROS-2 is a slightly shallower survey which translates to significantly lower signal-to-noise ratio lightcurves.

Key words: Magellanic Clouds – methods: data analysis – quasars: general

1 INTRODUCTION

Given the immense amount of data being produced by current deep-sky surveys such as Pan-STARRS (Kaiser et al. 2002), and future surveys such as LSST (Matter 2007) and SkyMapper (Keller et al. 2007), astronomy is facing new challenges on how to analyze *big data* and thus on how to search or predict events/patterns of interest.

The size of the data has already exceeded the capability of manual examination or the capability of standard data analysis tools. LSST will produce 15 terabytes of data per night, which is even beyond the capacity of typical data storage today.

Thus in order to analyze such a huge amounts of data and detect interesting events or patterns with minimum false positives, innovative and novel data analysis methods are crucial for the success of such surveys.

In our previous works (Kim et al. 2011a, 2012) we developed classification models for the selection of quasars from large photometric databases using variability characteristics as the main discriminators. In particular we used a supervised classification model trained using a set of variability features calculated from MACHO lightcurves (Al-

cock 2000). We applied the trained model to the entire MACHO database consisting of ~ 40 million lightcurves and selected few thousands of quasar candidates. In this paper, we present an improved classification model used to detect quasars on MACHO (Alcock 2000) and EROS-2 dataset (Tisserand et al. 2007). The new model which works over an extended set of variability features, substantially decreases false positive rate and increases efficiency.

The actual model improvement is a result of an improvement in the machine learning classification model and the lightcurve features we use. Machine learning classification methods have been very popular for many decades. These methods are data analysis models that learn to predict a categorical variable from a set of other variables (of any type). Most known classification models are: decision trees (Quinlan 1993), naive Bayes (Duda & Hart 1973), Neural Networks (Rumelhart et al. 1986), Support Vector Machines (Cortes & Vapnik 1995) and Random Forest (Breiman 2001). There are some meta-models to improve classification results like Boosting methods Freund & Schapire (1997) and Mixtures of Experts (Jordan 1994), among others. In general more recent classifiers are a result of research focused on building models able to search for

patterns within high dimensional datasets, where the combinatorial number of possible projections of data is large.

Many machine learning classifiers have been applied to the analysis of astronomical data in particular to classify transients and variable stars from time series data (Bloom et al. 2011; Richards et al. 2011; Bloom & Richards 2011; Debosscher et al. 2007; Wachman et al. 2009; Wang et al. 2010; Kim et al. 2011a,b). (Wang et al. 2010) proposed an algorithm to fit phase-shifted periodic time series using a mixture of Gaussian processes. (Debosscher et al. 2007) used many machine learning classifiers to learn a model that classifies variable stars in a sample from Hipparcos and OGLE databases. (Richards et al. 2011) used Random Forest classifier to classify between pulsational variables and eclipsing systems used in Milky Way tomography. In Bloom et al. (2011) they used machine learning algorithms to classify transients and variable stars from the Palomar Transient Factory (PTF) survey (Rau et al. 2009). In Wachman et al. (2009) they used cross correlation as a phase invariant feature to be used as a similarity indicator in a kernel function.

In this work we used a Random Forest classifier (Breiman 2001) boosted with the AdaBoost algorithm (Freund & Schapire 1997). The Random Forest classifier comes from the well-known decision tree model (Quinlan 1993) and Bagging techniques (Breiman 1996), where the model randomly explores several subsets of features while analyzing samples of training data. This model performs very well in many machine learning domains (Breiman 2001). AdaBoost algorithm (Freund & Schapire 1997) is a boosting technique which fits a sequence of classification models (in this case a sequence of many Random Forests) to different subsets of data objects (in our case lightcurves), generating a mixture of classifiers each one specialized in smaller areas of the feature space. We call these classifiers as “weak classifiers” or “simpler classifiers”. This is a nice property for quasar classification, given that there are only a few known training quasars compared with the amount of non-quasars lightcurves. Having some weak classifiers that take care of some areas with no training quasars helps to filter out many non-quasars, while other specialized classifiers perform well near the quasar areas in the feature space.

Besides improving the classification model, we added new features as descriptors of lightcurves. These features correspond to the parameters of the continuous auto regressive (CAR(1)) model (Belcher et al. 1994) fitted to the lightcurves. Previous work shows that describing quasars using CAR(1) fitting parameters gives suitable results to differentiate them from other classes of lightcurves (Kelly et al. 2009). In this work they did not use machine learning classifiers to automatically detect quasars, they use CAR(1) model to fit 100 quasars lightcurves in order to find correlations between CAR(1) parameters and luminosity characteristics.

In our work we show that by adding CAR(1) features to our previous set of features (used in Kim et al. (2011a)), we can learn more accurate models for quasar detection. Given that our model is built to find quasars over dozens of millions of stars, we need to be very efficient in the estimation of the optimal parameters in order to make the process feasible within a considerable amount of time. Unfortunately, methods such as Metropolis Hastings or Gibbs Sampling are

not suitable for our purposes, given the computational cost they involve.

To gain efficiency, we reduce the problem by approximating one of the parameters (the mean value of the light curve) and optimizing the remaining parameters (the amplitude and time scale of the variability) using a multi-dimensional unconstrained nonlinear minimization (Nelder & Mead 1965). Once we get the optimal parameters we use them as features of the object corresponding to the lightcurve. Besides the CAR(1) features we also used time series features as in our previous work (Kim et al. 2011b), in section 4 we give details about all the features we extracted.

To check the fitting accuracy of our model we first calculate the training accuracy of our classifier using 10-fold cross validation over a training set, which consists of about six thousand known light curves corresponding to different kinds of variable stars, non-variable stars and confirmed quasars; one set corresponding to the MACHO database and another to the EROS-2 database. In the MACHO case we substantially improve our training accuracy compared with our previous work (Kim et al. 2011b), increasing 14.3% in precision and 3.6% in recall for the MACHO database. In EROS-2 training database, we get about the same training efficiency as in the MACHO case but we could not compare to our previous work because this is the first time we attempt to classify in EROS-2 database. As an extra test for our candidates, we crossmatch them with the previous set of strong candidates found in Kim et al. (2011b), details are presented in section 5.

Using parallel computing we decrease the processing time to allow us to select quasar candidates from the entire database within three days. Note that the data analysis schema used in this work can be applied to any of the ongoing and future synoptic sky surveys such as Pan-STARRS, LSST, and SkyMapper, among others.¹

If confirmed the selected quasars from the MACHO database will provide critical information for galaxy evolution, black hole growth, large scale structure, etc. (Heckman et al. 2004; Bower et al. 2006; Trichas et al. 2009, 2010). Moreover the resulting quasar lightcurves will be a valuable dataset for quasar time variability studies, (e.g. time scale, blackhole mass, type i and ii variability) since MACHO and EROS lightcurves are well-sampled over 7.4 years (Alcock 2000).

The paper is organized as follows, in section 2 we present details about EROS-2 database, in section 3 we describe in details the classification model we use, including the Random Forest Model and AdaBoost, in section 4 we describe the features we use to describe the lightcurves, in section 5 we describe the experimental results for the MACHO and EROS-2 dataset.

2 EROS-2 DATASET

The EROS-2 collaboration made use of the MARLY telescope, a one meter diameter Ritchey-Chrétien ($f/5.14$) instrument dedicated to the survey. It was operated between

¹ Our main computer resource is The Odyssey cluster supported by the FAS Research Computing Group at Harvard.

July 1996 and March 2003 at La Silla Observatory (ESO, Chile). It was equipped with two wide angle CCD cameras which are located behind a dichroic beam-splitter. Each camera is a mosaic of 8 CCDs, 2 along right ascension and 4 along declination. Each CCD has 2048×2048 pixels of $15 \times 15 \mu\text{m}^2$ individual size, corresponding to a $0.6 \times 0.6 \text{ arcsec}^2$ pixel surface on the sky. The size of the field of view is 0.7° along right ascension and 1.4° along declination. The dichroic beam-splitter allowed simultaneous imaging in two broad non-standard passbands, B_E in the range 4200-7200 (the so-called “blue” channel), and R_E in the range 6200-9200 (the so-called “red” channel). The blue filter is intermediate between the standard V and R standard passbands, while the red filter is analogous to I_c . The normalized transmission curve of these filters, compared to standard ones, is given by Hamadache (2004)² on Fig. 3.3. Tisserand et al. (2007) give in Eq. (4) the equations to transform EROS-2 magnitudes into V and I_c ones within an accuracy of 0.1 magnitude.

The light curves of individual stars were constructed from fixed positions on templates using PEIDA, a software specifically developed for the photometry of EROS 2 images (Ansari 1996). The nomenclature of objects is defined as in Derue et al. (2002).

3 METHODOLOGY

To train a model that learns to detect quasars, we propose to use a combination of classifiers. Combination of multiple classifiers was first proposed by Xu et al. (1992). In that work, they proved that combining multiple classifiers overcome many of the individual classifiers limitations. In many pattern recognition problems, such as character recognition, handwritten text recognition and face recognition (Zhao et al. 2003; Plamondon & Srihari 2000), combination of multiple classifiers obtain much better classification performance. One effective way to combine classifiers is the AdaBoost algorithm, proposed in Freund & Schapire (1997).

The AdaBoost algorithm consists of a set of base classifiers that are trained sequentially, such that each classifier is trained on the instances where the previous classifier obtained a bad performance (learn what your partners could not learn). In Freund & Schapire (1997), they show that if the training set used for each classifier depends on the goodness of fit of the previous classifier, then the performance of the whole system improves. To make that the base classifiers focus on different subsets of the training set, we assign weights to training data instances. The lower the weight for an instance, the less the classifier focuses on it (see section 3.1 for further details).

One of the advantages of boosting methods is that after the model fitting phase is completed, each of the base classifiers become an expert in some subset of data objects. This is one of the main reasons that motivate us to use a previous boosting step. Given that we have a very small amount of known quasars in our training set compared with the amount of non quasars, training a set of base classifiers that just learn how to filter out some of the non quasars

would be very helpful for the next base classifier used in the sequential process. We now present a detailed description of the boosting method we use in this work, the AdaBoost algorithm (Freund & Schapire 1997).

3.1 AdaBoost Algorithm

AdaBoost, short for adaptive boosting, is a machine learning algorithm proposed by Freund and Schapire (Freund & Schapire 1997). It is a meta-algorithm because it combines many learning algorithms to perform classification. AdaBoost is adaptive in the sense that subsequent classifiers built are tweaked in favor of those instances misclassified by previous classifiers. Although AdaBoost is sensitive to noisy data and outliers, it is less susceptible to overfitting (Dietterich 1995) than most learning algorithms.

In the context of lightcurve-classification, suppose we have a training (labeled) set of n lightcurves and q features describing each lightcurve. Each lightcurve in the training set has a known given label (e.g. quasar or non-quasar). Let $[\mathbf{x}_1, \dots, \mathbf{x}_n]$ be a set of n descriptors where each \mathbf{x}_i $i \in [1 \dots n]$ is a vector associated to the lightcurve i where its descriptor (features) values are $\{x_{i1}, \dots, x_{iq}\}$ where q is the number of features. Let $\{y_1, \dots, y_n\}$ be the labels such that $y_i = 1$ if the lightcurve i is a quasar and $y_i = -1$ otherwise.

Let H be the set of m classifiers $\{h_1, \dots, h_m\}$, where $h_i : X \rightarrow Y$ and $D^{(t)}$ be the distribution of weights on classifiers at iteration t . Define m to be the number of classifiers and a constant T to be the number of times to iterate in the AdaBoost algorithm.

Initialization:

$$\begin{aligned} X &= [x_1, x_2, \dots, x_n] \\ Y &= [y_1, y_2, \dots, y_n] \\ D^{(1)} &= [d_1^{(1)}, d_2^{(1)}, \dots, d_n^{(1)}] := [\frac{1}{n}, \frac{1}{n}, \dots, \frac{1}{n}] \\ T &\leq n \end{aligned}$$

Algorithm:

```

for  $t = 1$  to  $T$  do
  for  $j = 1$  to  $m$  do
     $\epsilon_j := \sum_{i=1}^n d_i^{(t)} (1 - \delta_{y_i, h_j(x_i)})$ 
  end for
   $\epsilon_t := \min \epsilon_j$ 
  if  $\epsilon_t \geq 0.5$  then
    break
  end if
   $h_t := \operatorname{argmin}_{h_j \in H} \{\epsilon_j\}$ 
   $\alpha_t := \frac{1}{2} \ln((1 - \epsilon_t)/\epsilon_t)$ 
  for  $i = 1$  to  $n$  do
     $d_i^{(t+1)} := d_i^{(t)} \exp(-\alpha_t y_i h_t(x_i))/Z_t$ 
  end for
end for
 $\mathcal{H}(X) := [\mathcal{H}(x_1), \mathcal{H}(x_2), \dots, \mathcal{H}(x_n)]$ , such that
    
```

$$\mathcal{H}(x_i) = \operatorname{sign} \left(\sum_{t=1}^T \alpha_t h_t(x_i) \right)$$

² Available at URL: <http://tel.archives-ouvertes.fr>

- $\delta_{i,j}$ is the Kronecker delta.
- Z_t is a normalization factor

$$Z_t = \sum_{i=1}^n d_i^{(t)} \exp(-\alpha_t y_i h_t(x_i))$$

The equation to update the classifier weight distribution is constructed so that $-\alpha y_i h_t(x_i) < 1$ when $y_i = h_t(x_i)$ and $-\alpha y_i h_t(x_i) > 1$ when $y_i \neq h_t(x_i)$. Thus, after selecting an optimal classifier h_t , for the distribution D_t , the objects x_i that classifier h_t classified correctly are given less weight and those that it identified incorrectly are given more weight. Hence, when the algorithm proceeds to test the classifiers on $D^{(t+1)}$, it is more likely to select a classifier that better classifies the objects that h_t missed. Adaboost minimizes the training error (exponentially fast) if each weak classifier performs better than random guessing ($\epsilon_t < 0.5$).

The base classifier we used in this work is the Random Forest classifier (Breiman 2001), a very strong classifier that has shown very good results in many different domains. The following section shows details about the Random Forest classifier.

3.2 Random Forest Classifier

Random Forests (RF) is a popular and very efficient algorithm based on decision tree models (Quinlan 1993) and Bagging for classification problems (Breiman 1996, 2001). It belongs to the family of ensemble methods, appearing in machine learning literature at the end of nineties (Dietterich 2000) and has been used recently in the astronomical journals (Carliles et al. 2010; Richards et al. 2011). The process of training or building a Random Forest given training data is as follows:

- Let P be the number of trees in the Forest and F the number of features on each tree, both values are model parameters.
- Build P sets of n samples taken with replacement from the training set; this is called bagging. Note that each of the P bags has the same number of elements from the training set but less different examples, given that the samples are taken with replacement.
- For each of the P sets, train a decision tree using a random sample of F features from the set of q possible features.

The Random Forest classifier creates many linear separators inside many feature-subsets until it gets suitable separations between objects from different classes. Linear separations come from each decision tree, each of the feature-subsets come from the random feature selection process on each tree. The bagging procedure is very useful to estimate the error of the classifier during the training process. This error can be estimated using out-of-the-bag procedure, which means, “evaluate the performance of each tree using the objects not selected in the bag which belong to the tree” (see Breiman (2001) for further details).

After training the Random Forest, to classify a new unknown lightcurve descriptor, one uses each of the decision trees already trained with the Random Forest to classify the new unknown instance and the final decision is the most

voted class among the set of P decision trees (see Breiman (2001) for more details). In Breiman (2001) they show that as the number of trees tend to infinity the classification error of the RF becomes bounded and the classifier does not overfit the data.

4 FEATURE EXTRACTION

We extracted 14 features per each band for each lightcurve. Those features correspond to 11 time series features used in our previous work (Kim et al. 2011b) and 3 features corresponding to the CAR(1) process.

4.1 Time Series features

Here we very briefly summarize the 11 time series features used in our previous work (Kim et al. 2011b).

- N_{above}, N_{below} : Is the number of points above/below the upper/lower bound line calculated as points that are $\pm 4\sigma$ over the average of the autocorrelation functions.
- Stetson K_{AC} : Is the variability index derived based on the autocorrelation function of each lightcurve (Stetson 1996).
- R_{cs} : Is the range of the cumulative sums (starting from 1 to the number of observations) of each lightcurve (Ellaway 1978).
- σ/\bar{m} : The ratio of the standard deviation, σ , to the mean magnitude, \bar{m} .
- Period and Period S/N: Using Lomb-Scargle algorithm (Lomb 1976; Scargle 1982) we used the period with the highest value in the periodogram along with the signal to noise of the best period.
- Stetson L : Is a variability index (Stetson 1996) that describes the synchronous variability of different bands.
- η : Is the ratio of the mean of the square of successive differences to the variance of data points.
- $B - R$: Average color for each lightcurve
- Con : Is the number of three consecutive data points that are brighter or fainter than 2σ and normalized the number by $N - 2$.

4.2 Continuous Auto Regressive Process Features

We use continuous time auto regressive model (CAR(1)) to model irregular sampled time series in MACHO and EROS-2 lightcurves. CAR(1) process has three parameters, it provides a natural and consistent way of estimating a characteristic time scale and variance of lightcurves. CAR(1) process is described by the following stochastic differential equation (Brockwell & Davis 2002)

$$dX(t) = -\frac{1}{\tau}X(t)dt + \sigma_C\sqrt{dt}\epsilon(t) + bdt, \quad (1)$$

for $\tau, \sigma_C, t \geq 0$

where the mean value of the lightcurve $X(t)$ is $b\tau$ and the variance is $\frac{\tau\sigma_C^2}{2}$. τ is the relaxation time of the process $X(t)$, it can be interpreted as describing the variability amplitude of the time series. σ_C can be interpreted as describing the variability of the time series on time scales shorter than τ .

$\epsilon(t)$ is a white noise process with zero mean and variance equal to one. The likelihood function of a CAR(1) model for a lightcurve with observations $\mathbf{x} = \{x_1, \dots, x_n\}$ observed at times $\{t_1, \dots, t_n\}$ with measurement error variances $\{\delta_1^2, \dots, \delta_n^2\}$ is:

$$p(\mathbf{x}|b, \sigma_C, \tau) = \prod_{i=1}^n \frac{1}{[2\pi(\Omega_i + \delta_i^2)]^{1/2}} \exp\left\{-\frac{1}{2} \frac{(\hat{x}_i - x_i^*)^2}{\Omega_i + \delta_i^2}\right\} \quad (2)$$

$$x_i^* = x_i - b\tau \quad (3)$$

$$\hat{x}_0 = 0 \quad (4)$$

$$\Omega_0 = \frac{\tau\sigma_C^2}{2} \quad (5)$$

$$\hat{x}_i = a_i\hat{x}_{i-1} + \frac{a_i\Omega_{i-1}}{\Omega_{i-1} + \delta_{i-1}^2}(x_{i-1}^* + \hat{x}_{i-1}) \quad (6)$$

$$\Omega_i = \Omega_0(1 - a_i^2) + a_i^2\Omega_{i-1} \left(1 - \frac{\Omega_{i-1}}{\Omega_{i-1} + \delta_{i-1}^2}\right) \quad (7)$$

$$a_i = e^{-(t_i - t_{i-1})/\tau} \quad (8)$$

To find the optimal parameters we maximize the likelihood with respect to σ_C , b and τ . Given that the likelihood does not have an analytical solution, we can solve it with a statistical sampling method such Metropolis Hastings (Metropolis et al. 1953). Given that we extract features for all the lightcurves in EROS-2 and MACHO datasets (about 28 and 40 millions of stars respectively), performing a statistical sampling process to determine the optimal parameters would be feasible only in cases where stable solutions are found in a reasonable amount of time. We consider that less than 3 seconds is reasonable given our hardware resources. Unfortunately we could not get stable solutions considering that restriction. To overcome this situation we simplify the optimization problem by reducing the number of parameters to be estimated. Instead of estimating σ_C , b and τ , we just estimate σ_C and τ and then we calculate b as the mean magnitude of the lightcurve divided by τ . To check that this estimation works well, we use a sample of 250 lightcurves and compare the reduced Chi-square error using two and three parameters optimization, getting differences smaller than 2.5% in average.

This approximation allows us to perform a two dimensional optimization which can be solved with a regular numerical method in less than one second per lightcurve. We used the Nelder-Mead multidimensional unconstrained non-linear optimization (Nelder & Mead 1965) to find the optimal parameters. Figure 1 shows the fitting of three quasar lightcurves with the resulting CAR(1) coefficients using the Nelder-Mead algorithm. Note that instead of using b directly as a feature, we use the mean magnitude of the lightcurve (\bar{m}), in order to have a cleaner feature (b is calculated from τ , which is already used as a feature).

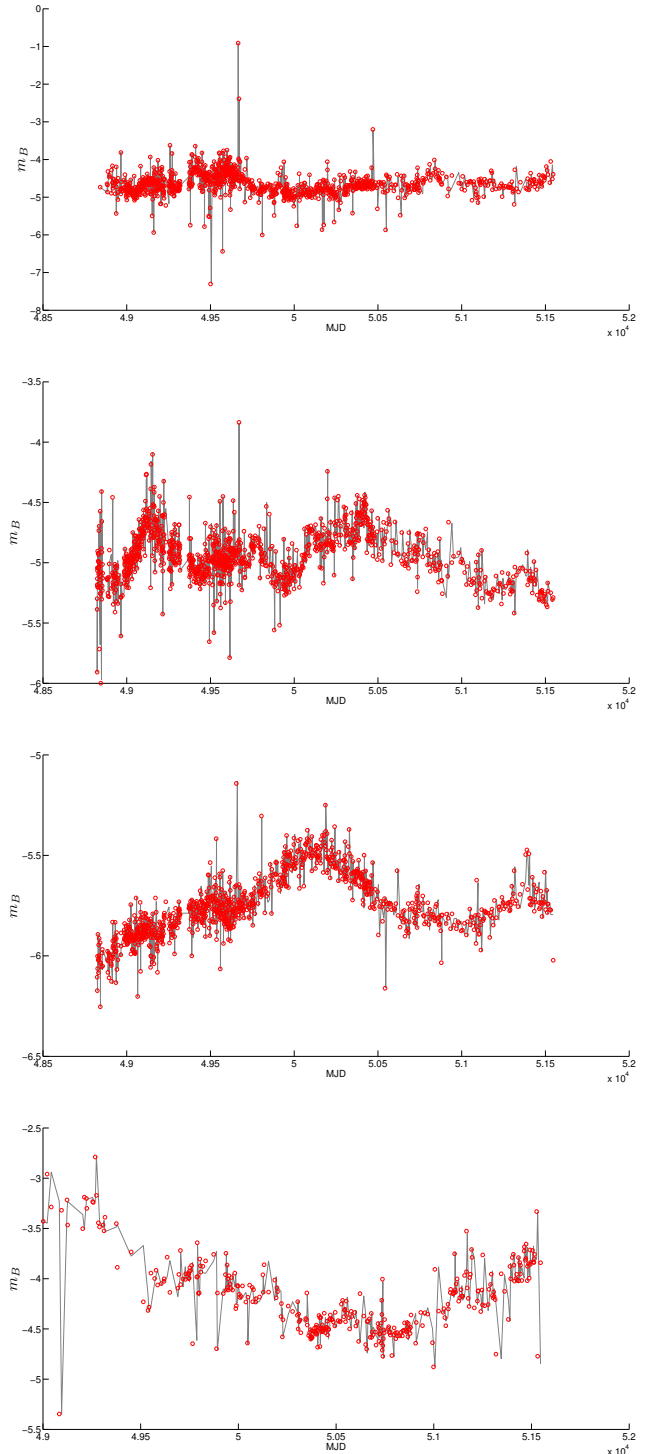


Figure 1. Quasar lightcurves (red circles) fitted with optimal CAR(1) model (gray lines) using Nelder-Mead.

5 QSO CANDIDATES ON EROS-2 AND MACHO DATASETS

5.1 EROS-2 dataset

To train a model able to find quasars in EROS-2 we create a training set composed of 65 known quasars, 67 Be stars,

330 Long Periodic stars, 5829 non-variable stars, 1727 RR Lyrae, 406 Cepheids, and 488 EB stars. We get these stars cross-matching the EROS-2 dataset with MACHO known stars using positional matching with 3 arcsec of accuracy. We extracted features in bands R and B. Figures 2 and 3 show projections of the training set on different sets of features containing CAR(1) features. In many cases is easy to get a natural separation between quasars and the variable stars, but usually quasars overlap many of the non variable stars (ex. σ_C with B - R, σ_C with τ , \bar{m} with τ). Fortunately, there are many projections where quasars and non-variable stars are mostly separated, (ex. σ_C with *Con*, σ_C with \bar{m} , σ_C with Stetson K_{AC} , τ with R_{cs} , τ with Stetson K_{AC} .)

To compare the distribution of the objects predicted as quasars with the training quasars and other variable stars, we plot our EROS-2 training data plus the predicted quasars projected on many different pairs of features (Figs. 4 , 5). We can see that in most of the cases Predicted quasars and Training quasars have very similar distributions regardless of the small amount of training quasars we use. Main differences between both distributions are in general because of the big difference in size comparing training and testing data, resulting in a set of predicted quasars ~ 20 times bigger than the training quasars set.

To get an indicator of the accuracy in the training set on EROS-2 dataset, we run a 10 fold cross validation. This validation method consists of partitioning the dataset in 10 folds (subsets) of the same size, we iterate 10 times, on iteration k we train the classifier with all the folds but the fold k , then we test the performance on the fold k (the one which the model did not see during the training). The process returns the model prediction for the entire dataset (the union of the 10 testing folds is equal to the data). We measure the accuracy using the *F-score* indicator. This indicator is calculated as the harmonic mean of precision and recall:

$$F\text{-Score} = 2 \times \frac{\text{precision} \times \text{recall}}{\text{precision} + \text{recall}}$$

Where precision and recall are defined as:

$$\text{precision} = \frac{tp}{tp+fp} \quad \text{recall} = \frac{tp}{tp+fn}$$

Where tp , fp and fn are the number of true positives, false positives and false negatives respectively.

Table 1 show the results for the boosted version of Random Forest, regular Random Forest and SVM (classifier used in our previous work (Kim et al. 2011b)) with and without CAR features.

We find 1160 candidates in the EROS-2 dataset. To validate our candidates we crossmatch them with the list of 663 MACHO strong candidates in Kim et al. (2011b). From that list, only 332 objects exists in EROS-2 dataset, we find 191 matches between our EROS-2 candidates and those 332 objects. Figure 6 shows some of the lightcurves of the quasar candidates for the EROS-2 dataset.

Regarding the efficiency in the extraction of the CAR(1) features and the time series features, we implemented parallel processing in order to perform the features extraction and classification in a reasonable amount of time. EROS-2 and MACHO databases are stored as a set of thousands of

Table 1. *F-score* for the EROS-2 training set using 10-fold cross validation for different classification models. Each classifiers is tuned with the optimal set of parameters. We can see that the boosted version of Random Forest with CAR features outperforms other classification models. In all cases using CAR features improves the result of the corresponding classifier.

SVM No CAR	SVM CAR	RF No CAR	RF CAR	AB+RF No CAR	AB+RF CAR
0.74	0.855	0.787	0.813	0.81	0.868

folders where each folder contains thousands of lightcurves of a given field. The feature extraction process runs as a set of parallel threads that run over different compressed files at the same time, extracting them and processing the lightcurves to get the features. Once the features are calculated they are written into a common file related to a particular folder, so each compressed file has a corresponding data file that stores the feature values of all the lightcurves within the folder. After the feature extraction process we run a classification process that runs in parallel over the thousands of data feature files calculated in the previous step.

5.2 MACHO dataset

MACHO was a survey which observed the sky starting in July 1992 and ending in 1999 to detect microlensing events produced by Milky Way halo objects. Several tens of millions of stars were observed in the Large Magellanic Cloud (LMC), Small Magellanic Cloud (SMC) and Galactic bulge (Alcock 2000).

For the MACHO dataset we built a training set composed of 3969 non-variable stars, 127 Be stars, 78 Cepheids, 193 eclipsing binaries, 288 RR Lyrae, 574 microlensing, 359 long-period variables, and 58 quasars. We get the variable stars from the list of known MACHO variable sources extracted from SIMBAD's MACHO variable catalog³ (Alcock 2001) and also from several other literature sources (Alcock 1997a,b; Wood 2000; Keller et al. 2002; Thomas 2005). To get the non variable stars, we randomly chose a subset of MACHO lightcurves from a few MACHO LMC fields and removed all the known MACHO variables from the subset.

Each lightcurve is described as a feature vector which contains 28 features, 14 features for band B and 14 features for band R as described in section 4.

Figures 7 and 8 show the training set projected on a two variables feature space. We can see that σ_C and τ features show separations between two groups of classes: i) non-variables, Cepheid and Eclipsing Binaries stars and ii) quasars, Microlensings, LPVs and Be stars. Combining \bar{m} and τ we can see a cluster of quasars, which overlaps with some of the Be stars, non-variables, Microlensing and long period variables, but separates very well quasars from Cepheids, Eclipsing Binaries stars and most of the non-variables. Projecting on σ_C and \bar{m} we can see that quasars separates from LPVs, Cepheids, Eclipsing Binaries, most of Be stars, most of the Microlensings and most of the non-variables. The biggest overlap is with Microlensings.

³ <http://vizier.u-strasbg.fr/viz-bin/VizieR?-source=II/247>

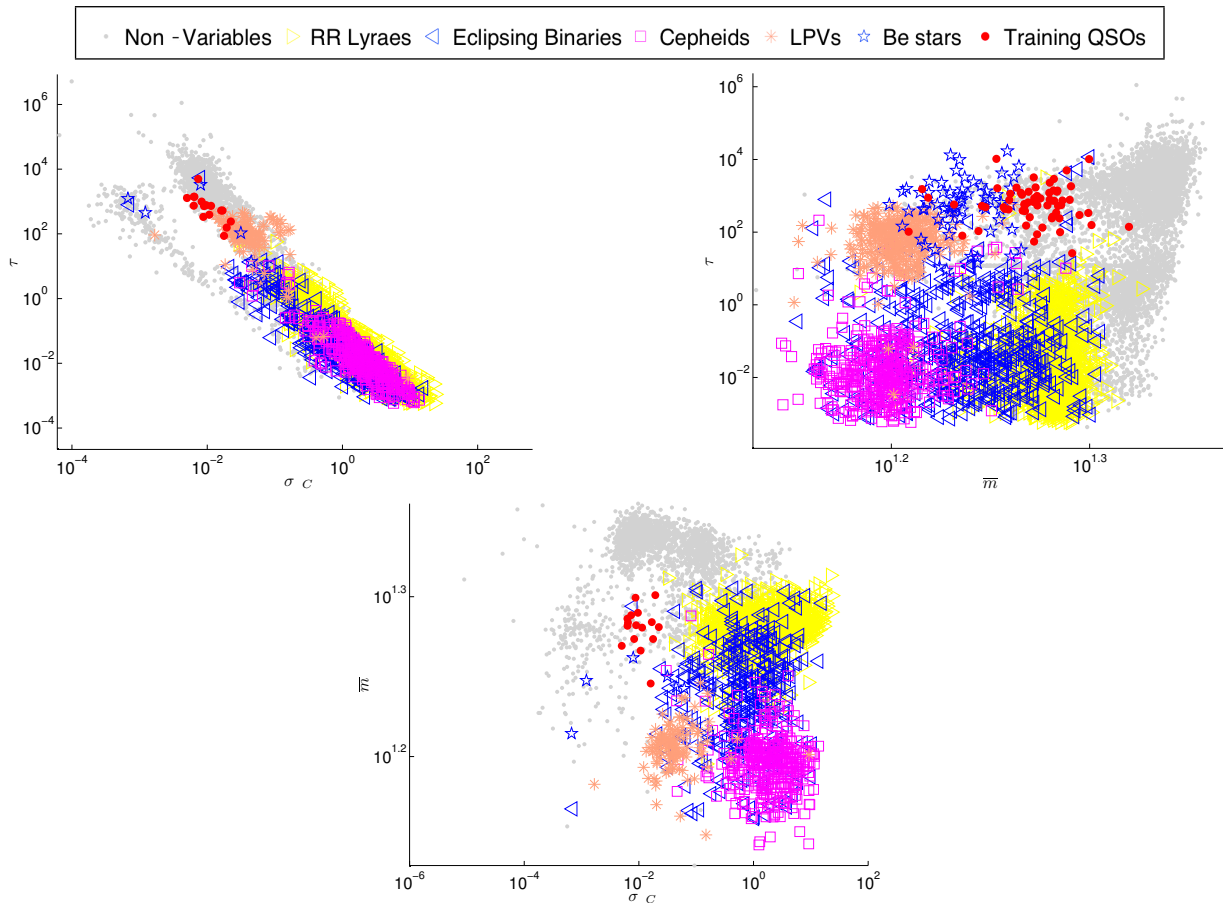


Figure 2. Projections on different pairs of CAR(1) features for EROS-2 training data

Table 2. F-Score for the MACHO training set using 10-fold cross validation for different classification models. Each classifier is tuned with the optimal set of parameters. We can see that the boosted version of Random Forest with CAR features outperforms other classification models. In all cases using CAR features improves the result of the corresponding classifier.

SVM No CAR	SVM CAR	RF No CAR	RF CAR	AB+RF No CAR	AB+RF CAR
0.787	0.824	0.826	0.841	0.844	0.877

By examining these projections we can see that quasars are clustered in high values of τ , with higher values compared to Eclipsing Binaries, Cepheids and RR Lyraes. σ_C is very good to separate quasars from non-variables, also from Cepheids, RR Lyraes and Eclipsing Binaries stars. σ_C is not a good feature to separate quasars from Microlensings, Be stars and LPVs, but combining σ_C with $B - R$ we get a strong separation between them.

Table 2 shows comparative results among different classification models. We included a Support Vector Machine, Random Forest and Random Forest Boosted with AdaBoost. On each case the classifier is tuned with the optimal set of parameters.

After we select and fit the model to the training set, we run on the whole MACHO data (about 40 million of

lightcurves), from where we get 2551 quasar candidates. We crossmatch our candidates with the 2566 and 663 strong candidates in our previous work (Kim et al. 2011b) getting 1148 and 494 matches respectively.

Figure 9 shows some of the new candidates we find that are not in the previous list for MACHO candidates in Kim et al. (2011b)

There are some cases where the model confuses a periodic star with a quasar. Figure 10 shows one example of this case.

To analyze the distribution of predicted quasars in the feature space we show some projections of the training data plus the predicted quasars. Figures 11 and 12 show the distribution of predicted quasars, training quasars and all the other classes of stars. As in the EROS-2 case, we can see that in many cases the predicted quasars show similar distributions compared with training quasars. There are some cases where a big portion of the predicted quasars is expanded out of the concentrated cluster of training quasars, for example, combining σ_C and $B - R$.

6 SUMMARY

In this work we present a new list of candidate quasars from MACHO and EROS-2 datasets. This new list is obtained using a new model that uses continuous auto correlation features plus time series features to feed a boosted version

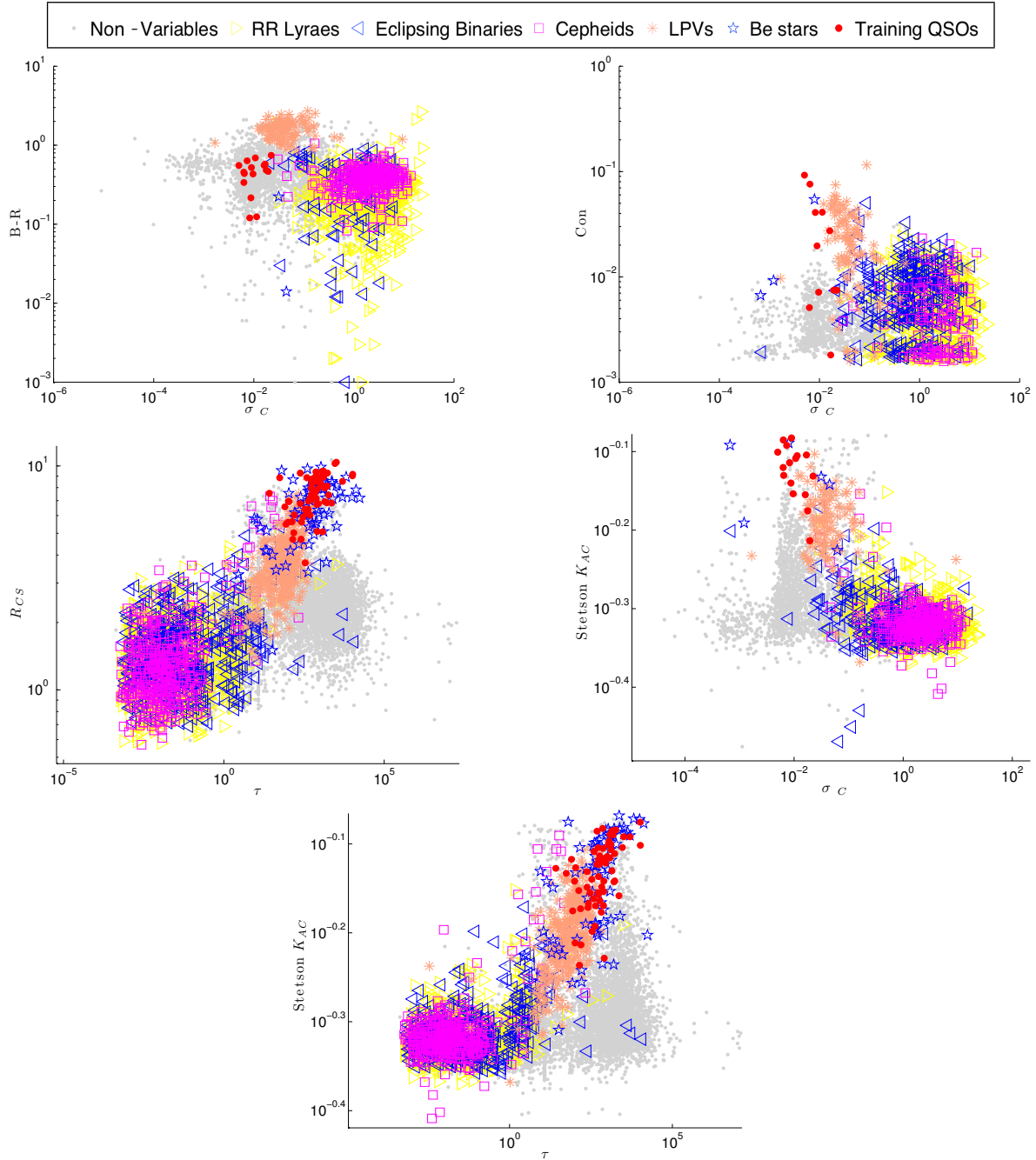


Figure 3. Projections on different pairs of features, combining CAR(1) features with time series features for EROS-2 training data

of the Random Forest classifier (Breiman 2001). With this model we obtain a list of 1160 candidates for the EROS-2 and 2551 candidates for the MACHO dataset. From our MACHO candidates we crossmatch them with the old list of candidates from Kim et al. (2011b) and we get 1148 matches. We crossmatch our EROS-2 candidates with the list of 663 MACHO strong candidates in Kim et al. (2011b). From that list, only 332 objects exist in the EROS-2 dataset, and we find 131 matches between our EROS-2 candidates and those 332 objects (see table 3). We prove that using boosted Random Forest with CAR(1) features we improve the fitting of

the model to the training set in both EROS-2 and MACHO datasets.

We show that quasars are well separated from many other kind of variable stars using CAR(1) features combined with time series features. We also proved that adding CAR(1) features, SVM, Random Forest and Boosted Random Forest improve their training accuracy. There are some challenges to overcome in future work such as the confusion of some periodic stars with quasars. We notice that about 25% of false positives correspond to periodic stars. We believe that adding a dedicated module to filter periodic stars we can improve the results.

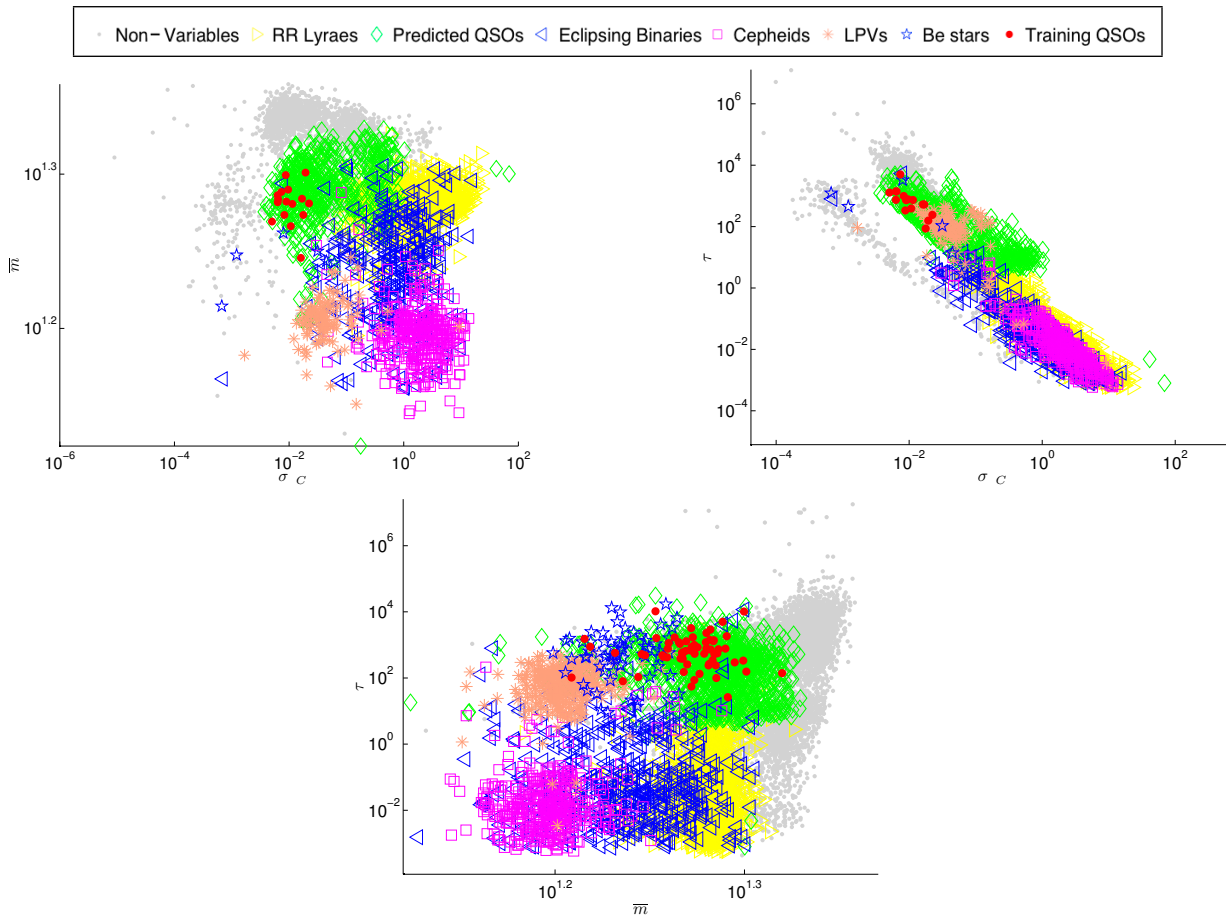


Figure 4. Predicted quasars and Training stars distributions projected on different pairs of CAR(1) features for EROS-2 data.

Previous Candidates MACHO (M_1)	Previous Strong Candidates MACHO (M_2)	New list of MACHO Candidates (M_3)	List of EROS-2 Candidates (E_1)
2566	663	2551	1160
Matches between (M_3) and (M_1)	Matches between (M_3) and (M_2)	Objects from (M_2) Catalogued in EROS-2	Matches between (ME) and (E_1)
1148	491	332 (ME)	131

Table 3. Table summarizing crossmatching results between different lists of quasars candidates

ACKNOWLEDGMENTS

This paper utilizes public domain data obtained by the MACHO Project, jointly funded by the US Department of Energy through the University of California, Lawrence Livermore National Laboratory under contract No. W-7405-Eng-48, by the National Science Foundation through the Center for Particle Astrophysics of the University of California under cooperative agreement AST-8809616, and by the Mount Stromlo and Siding Spring Observatory, part of the Australian National University. The analysis in this paper has been done using the Odyssey cluster supported by the FAS Research Computing Group at Harvard. This research has made use of the SIMBAD database, operated at CDS, Strasbourg, France. We thank everyone from the EROS-2 collaboration for the

access granted to the database. The EROS-2 project was funded by the CEA and the CNRS through the IN2P3 and INSU institutes.

This paper has been typeset from a $\text{T}_{\text{E}}\text{X}/\text{L}^{\text{A}}\text{T}_{\text{E}}\text{X}$ file prepared by the author.

REFERENCES

- Alcock, C., e. a. 1997a, ApJ, 491, L11+
- . 1997b, ApJ, 479, 119
- . 2000, ApJ, 542, 281
- . 2001, Variable Stars in the Large Magellanic

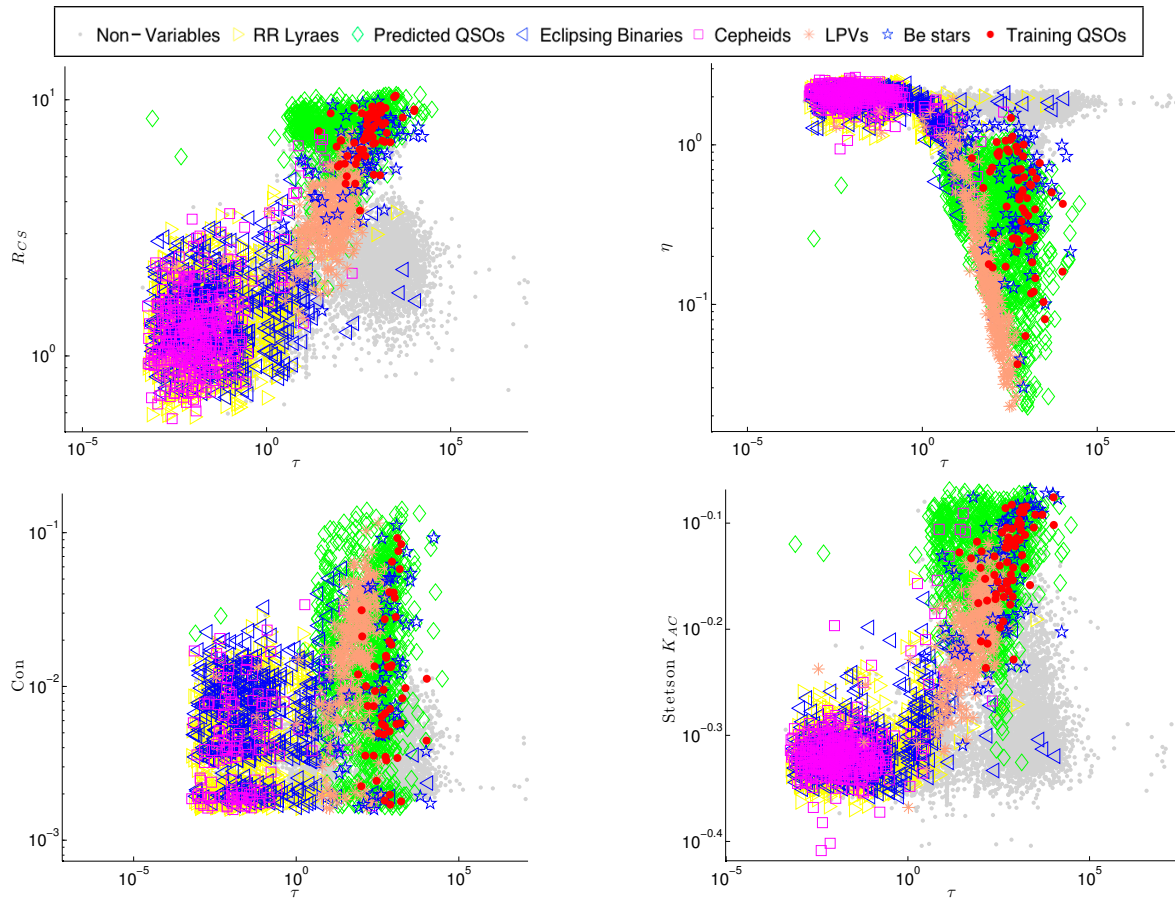


Figure 5. Predicted quasars and training stars distributions for τ combined with three time series features for EROS-2 data.

Clouds, VizieR Online Data Catalog (<http://vizier.u-strasbg.fr/viz-bin/VizieR?-source=II/247>)

Ansari, R. 1996, *Vistas in Astronomy*, 40, 519

Belcher, J., Hampton, J. S., & Wilson, G. T. 1994, *Journal of the Royal Statistical Society. Series B (Methodological)*, 56, 141

Bloom, J. S., & Richards, J. W. 2011, ArXiv e-prints

Bloom, J. S., Richards, J. W., Nugent, P. E., Quimby, R. M., Kasliwal, M. M., Starr, D. L., Poznanski, D., Ofek, E. O., Cenko, S. B., Butler, N. R., Kulkarni, S. R., Gal-Yam, A., & Law, N. 2011, ArXiv e-prints

Bower, R. G., Benson, A. J., Malbon, R., Helly, J. C., Frenk, C. S., Baugh, C. M., Cole, S., & Lacey, C. G. 2006, *MNRAS*, 370, 645

Breiman, L. 1996, in *Machine Learning*, 123–140

Breiman, L. 2001, in *Machine Learning*, 5–32

Brockwell, P., & Davis, R. 2002, *Introduction to Time Series and Forecasting* (Springer New York)

Carliles, S., Budavri, T., Heinis, S., Priebe, C., & Szalay, A. 2010, *The Astrophysical Journal*, 712, 511

Cortes, C., & Vapnik, V. 1995, *Machine Learning*, 20, 273

Debosscher, J., Sarro, L., Aerts, C., Cuypers, J., Vandebussche, B., Garrido, R., & Solano, E. 2007, *Astronomy and Astrophysics*, 475, 1159

Derue, F., Marquette, J.-B., Lupone, S., Afonso, C., Alard, C., Albert, J.-N., Amadon, A., Andersen, J., Ansari, R., Aubourg, É., Bareyre, P., Bauer, F., Beaulieu, J.-

P., Blanc, G., Bouquet, A., Char, S., Charlot, X., Couchot, F., Coutures, C., Ferlet, R., Fouqué, P., Glicenstein, J.-F., Goldman, B., Gould, A., Graff, D., Gros, M., Haassinski, J., Hamilton, J.-C., Hardin, D., de Kat, J., Kim, A., Lasserre, T., Le Guillou, L., Lesquoy, É., Loup, C., Magneville, C., Mansoux, B., Maurice, É., Milsztajn, A., Moniez, M., Palanque-Delabrouille, N., Perdureau, O., Prévot, L., Regnault, N., Rich, J., Spiro, M., Vidal-Madjar, A., Vigroux, L., Zylberajch, S., & EROS Collaboration. 2002, *Astronomy and Astrophysics*, 389, 149

Dietterich, T. 1995, *ACM Computing Surveys*, 27, 326

Dietterich, T. 2000, in *Proceedings of the First International Workshop on Multiple Classifier Systems* (Springer Verlag), 1–15

Duda, R., & Hart, P. 1973, *Pattern Classification and Scene Analysis* (John Wiley & Sons)

Ellaway, P. 1978, *Electroencephalography and Clinical Neurophysiology*, 45, 302

Freund, Y., & Schapire, R. 1997, *Journal of Computer and System Sciences*

Hamadache, C. 2004, PhD thesis, Université Louis Pasteur - Strasbourg I

Heckman, T. M., Kauffmann, G., Brinchmann, J., Charlot, S., Tremonti, C., & White, S. D. M. 2004, *ApJ*, 613, 109

Jordan, M. I. 1994, *Neural Computation*, 6, 181

Kaiser, N., Aussel, H., Burke, B. E., Boesgaard, H., Chambers, K., Chun, M. R., Heasley, J. N., Hodapp, K.-W.,

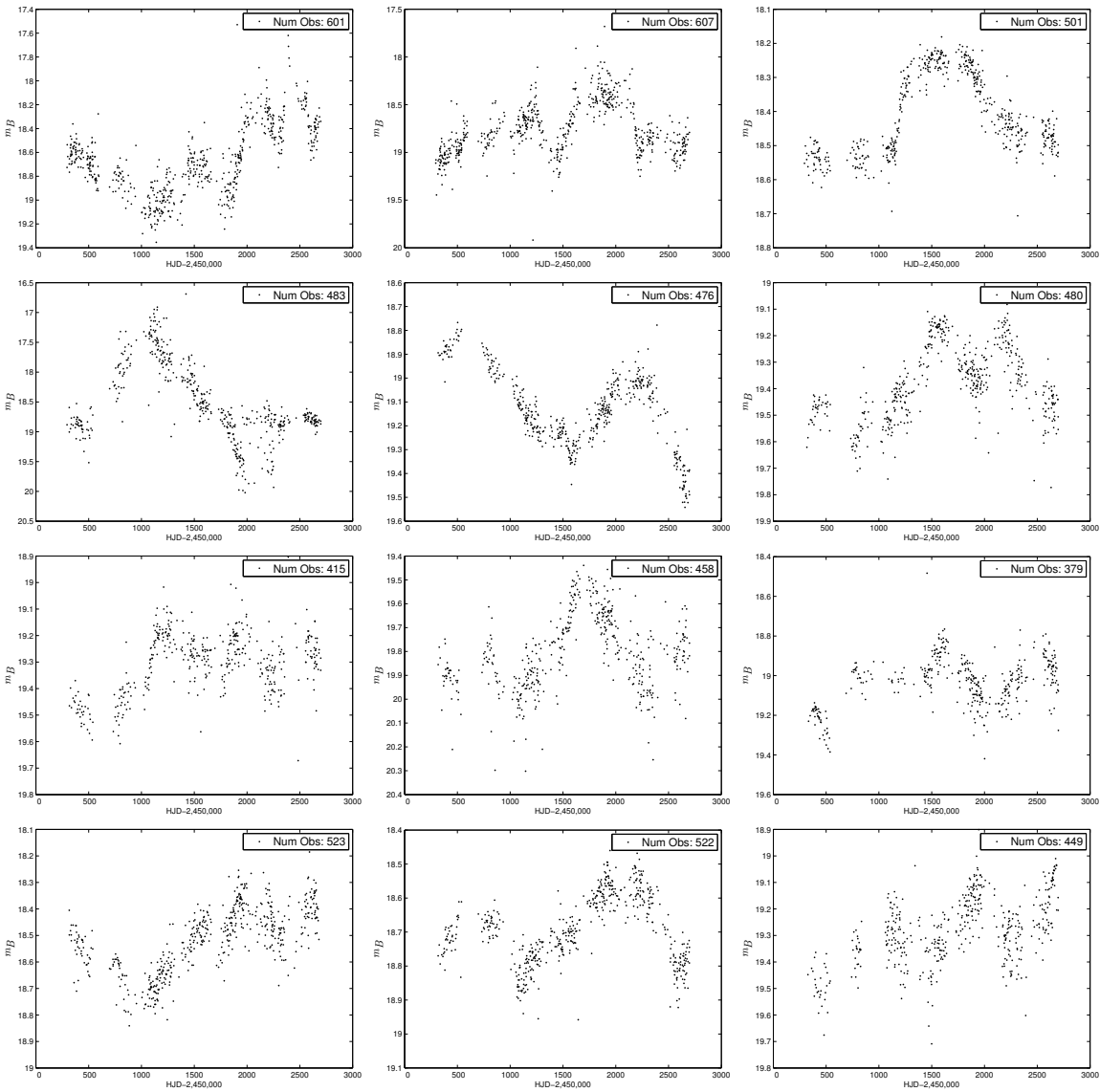


Figure 6. Lightcurves of quasar candidates predicted on EROS-2 dataset

Hunt, B., Jedicke, R., Jewitt, D., Kudritzki, R., Luppino, G. A., Maberry, M., Magnier, E., Monet, D. G., Onaka, P. M., Pickles, A. J., Rhoads, P. H. H., Simon, T., Szalay, A., Szapudi, I., Tholen, D. J., Tonry, J. L., Waterson, M., & Wick, J. 2002, in Society of Photo-Optical Instrumentation Engineers (SPIE) Conference Series, Vol. 4836, Society of Photo-Optical Instrumentation Engineers (SPIE) Conference Series, ed. J. A. Tyson & S. Wolff, 154–164

Keller, S. C., Bessell, M. S., Cook, K. H., Geha, M., & Syphers, D. 2002, *AJ*, 124, 2039

Keller, S. C., Schmidt, B. P., Bessell, M. S., Conroy, P. G., Francis, P., Granlund, A., Kowald, E., Oates, A. P., Martin-Jones, T., Preston, T., Tisserand, P., Vaccarella, A., & Waterson, M. F. 2007, *Publications of the Astronomical Society of Australia*, 24

Kelly, B. C., Bechtold, J., & Siemiginowska, A. 2009, 698, 895

Kim, D.-W., Protopapas, P., Byun, Y.-I., Alcock, C., Khardon, R., & Trichas, M. 2011a, 735

—. 2011b, *ApJ*, 735, 68

Kim, D.-W., Protopapas, P., Trichas, M., Rowan-Robinson, M., Khardon, R., Alcock, C., & Byun, Y.-I. 2012, 747

Lomb, N. R. 1976, *Ap&SS*, 39, 447

Matter, D. 2007, *Science*, 1

Metropolis, N., Rosenbluth, A., Rosenbluth, M., Teller, A., & Teller, E. 1953, *Journal of Chemical Physics*, 21, 1087

Nelder, J., & Mead, R. 1965, *Computer Journal*, 7, 308

Plamondon, R., & Srihari, S. 2000, *Pattern Analysis and Machine Intelligence*, *IEEE Transactions on*, 22, 63

Quinlan, J. 1993, *C4.5: programs for machine learning* (Morgan Kaufmann Publishers Inc.)

Rau, A., Kulkarni, S. R., Law, N. M., Bloom, J. S., Ciardi, D., Djorgovski, G. S., Fox, D. B., Gal-Yam, A., Grillmair, C. C., Kasliwal, M. M., Nugent, P. E., Ofek, E. O., Quimby, R. M., Reach, W. T., Shara, M., Bildsten, L., Cenko, S. B., Drake, A. J., Filippenko, A. V., Helfand, D. J., Helou, G., Howell, D. A., Poznanski, D., & Sullivan, M. 2009, *Publications of the Astronomical Society of*

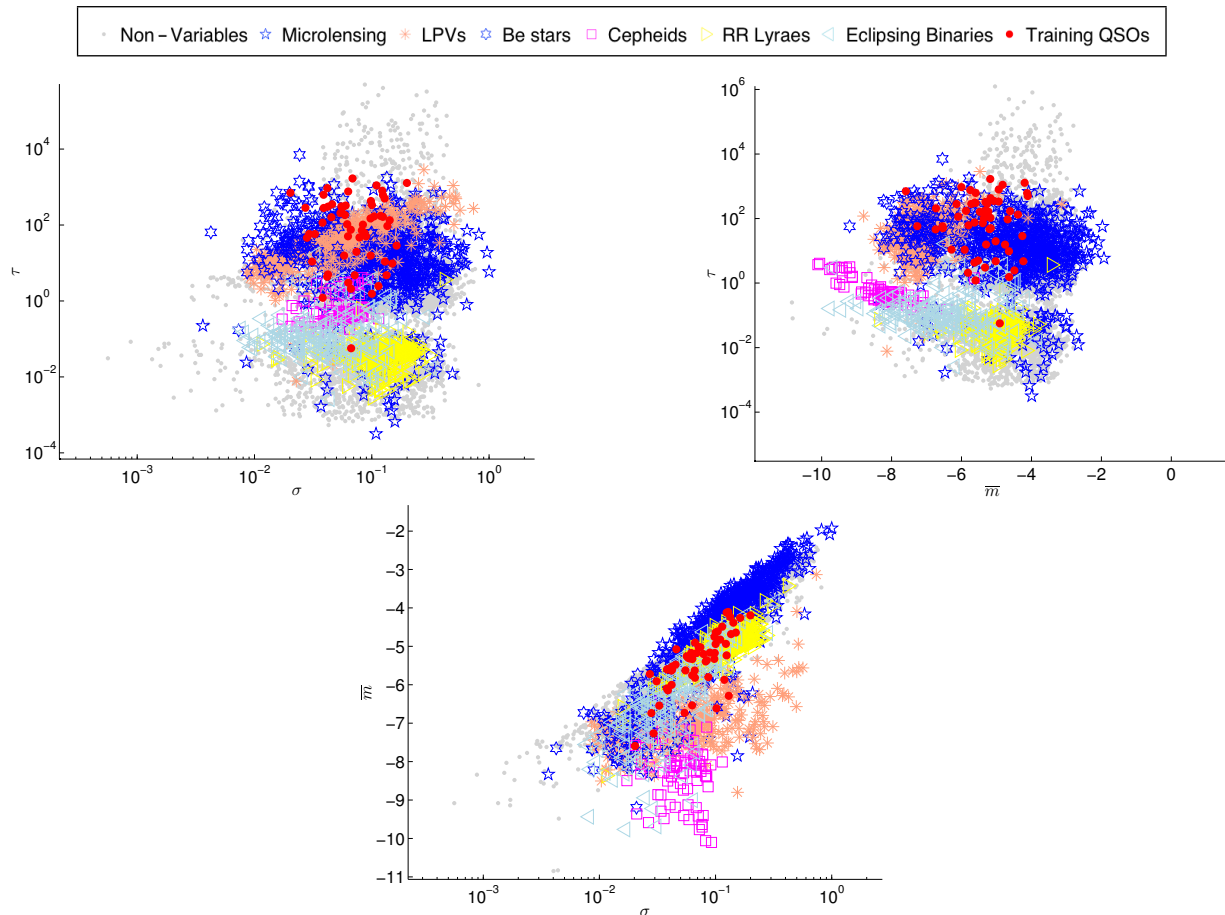


Figure 7. Training set projected on different pairs of CAR(1) features for MACHO data.

- the Pacific, 121, 1334
- Richards, J. W., Starr, D. L., Butler, N. R., Bloom, J. S., Brewer, J. M., Crellin-Quick, A., Higgins, J., Kennedy, R., & Rischard, M. 2011, *The Astrophysical Journal*, 733
- Rumelhart, D., Hinton, G., & Williams, R. 1986, *Learning internal representations by error propagation* (MIT Press), 318–362
- Scargle, J. D. 1982, *ApJ*, 263, 835
- Stetson, P. B. 1996, *PASP*, 108, 851
- Thomas, C. L., e. a. 2005, *ApJ*, 631, 906
- Tisserand, P., Le Guillou, L., Afonso, C., Albert, J. N., Andersen, J., Ansari, R., Aubourg, É., Bareyre, P., Beaulieu, J. P., Charlot, X., Coutures, C., Ferlet, R., Fouqué, P., Glencstein, J. F., Goldman, B., Gould, A., Graff, D., Gros, M., Haissinski, J., Hamadache, C., de Kat, J., Lasserre, T., Lesquoy, É., Loup, C., Magneville, C., Marquette, J. B., Maurice, É., Maury, A., Milsztajn, A., Moniez, M., Palanque-Delabrouille, N., Perdureau, O., Rahal, Y. R., Rich, J., Spiro, M., Vidal-Madjar, A., Vigroux, L., Zylberajch, S., & EROS-2 Collaboration. 2007, *Astronomy and Astrophysics*, 469, 387
- Trichas, M., Georgakakis, A., Rowan-Robinson, M., Nandra, K., Clements, D., & Vaccari, M. 2009, *MNRAS*, 399, 663
- Trichas, M., Rowan-Robinson, M., Georgakakis, A., Valtchanov, I., Nandra, K., Farrah, D., Morrison, G., Clements, D., & Waddington, I. 2010, *MNRAS*, 405, 2243
- Wachman, G., Khardon, R., Protopapas, P., & Alcock, C. 2009, in *Lecture Notes in Computer Science*, Vol. 5782, *Machine Learning and Knowledge Discovery in Databases*, ed. W. Buntine, M. Grobelnik, D. Mladenic, & J. Shawe-Taylor (Springer Berlin / Heidelberg), 489–505
- Wang, Y., Khardon, R., & Protopapas, P. 2010, in *Lecture Notes in Computer Science*, Vol. 6323, *Machine Learning and Knowledge Discovery in Databases* (Springer Berlin / Heidelberg), 418–434
- Wood, P. R. 2000, *Publications of the Astronomical Society of Australia*, 17, 18
- Xu, L., Krzyzak, A., & Suen, C. 1992, *Systems, Man and Cybernetics*, *IEEE Transactions*, 22, 418
- Zhao, W., Chellappa, R., Phillips, P. J., & Rosenfeld, A. 2003, *ACM Comput. Surv.*, 35, 399

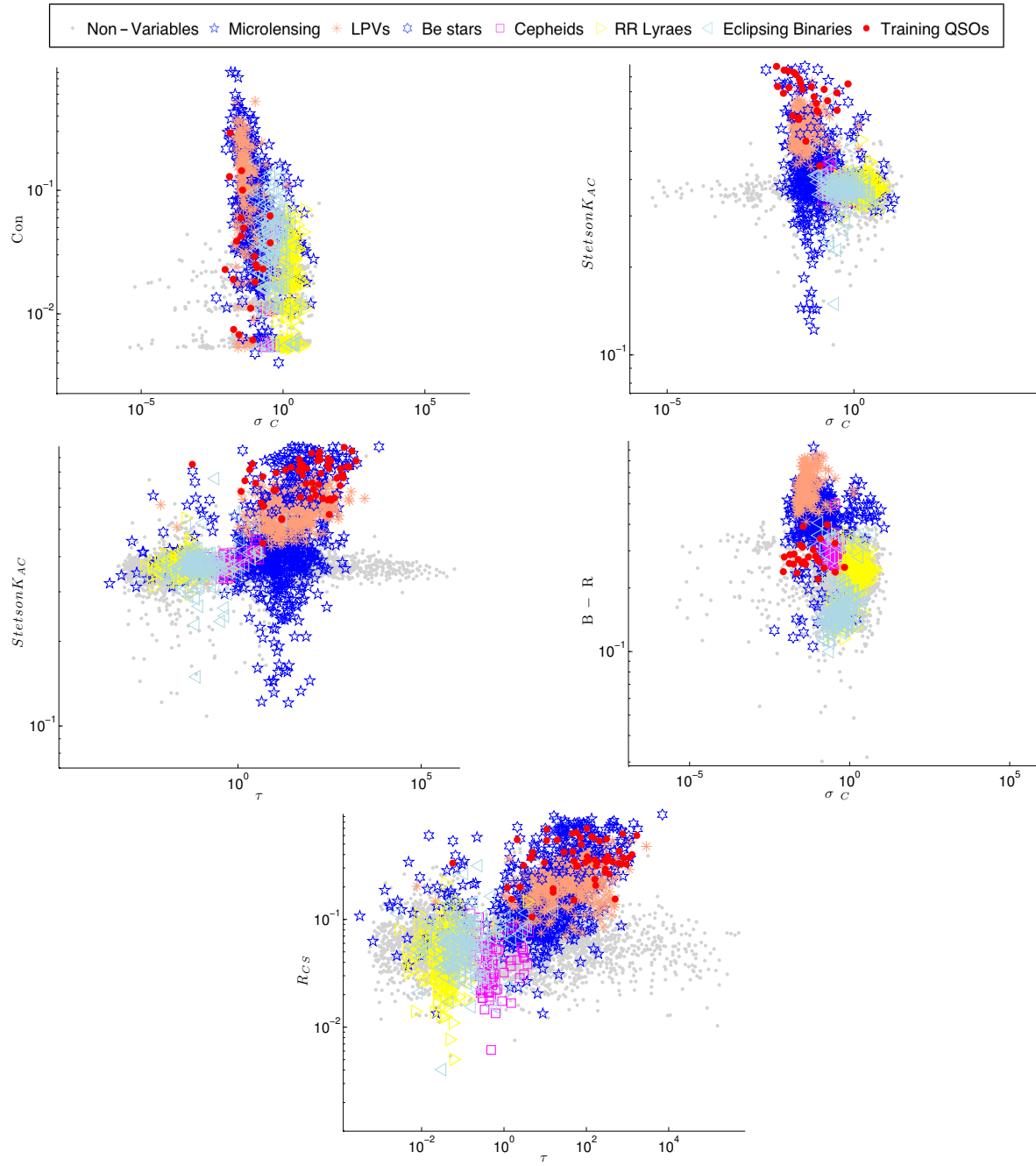


Figure 8. Projections on different pairs of features, combining CAR(1) features with time series features for MACHO training data

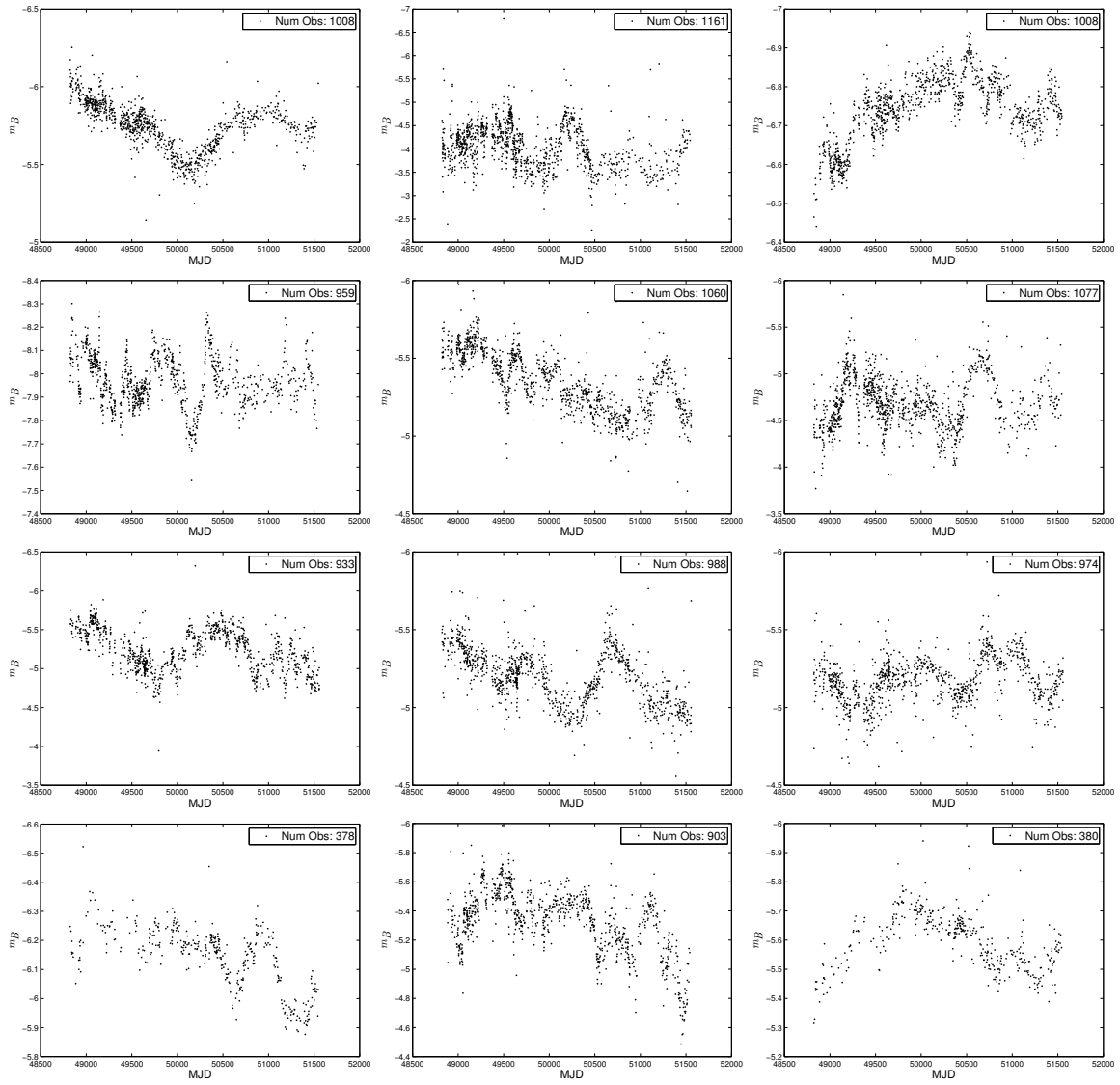


Figure 9. Lightcurves of new quasars candidates predicted from MACHO dataset

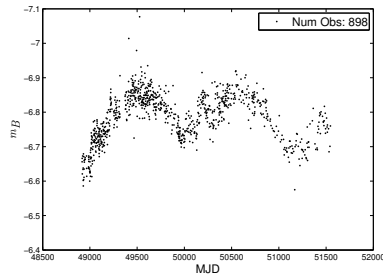


Figure 10. Lightcurve of a wrongly predicted quasar in MACHO dataset

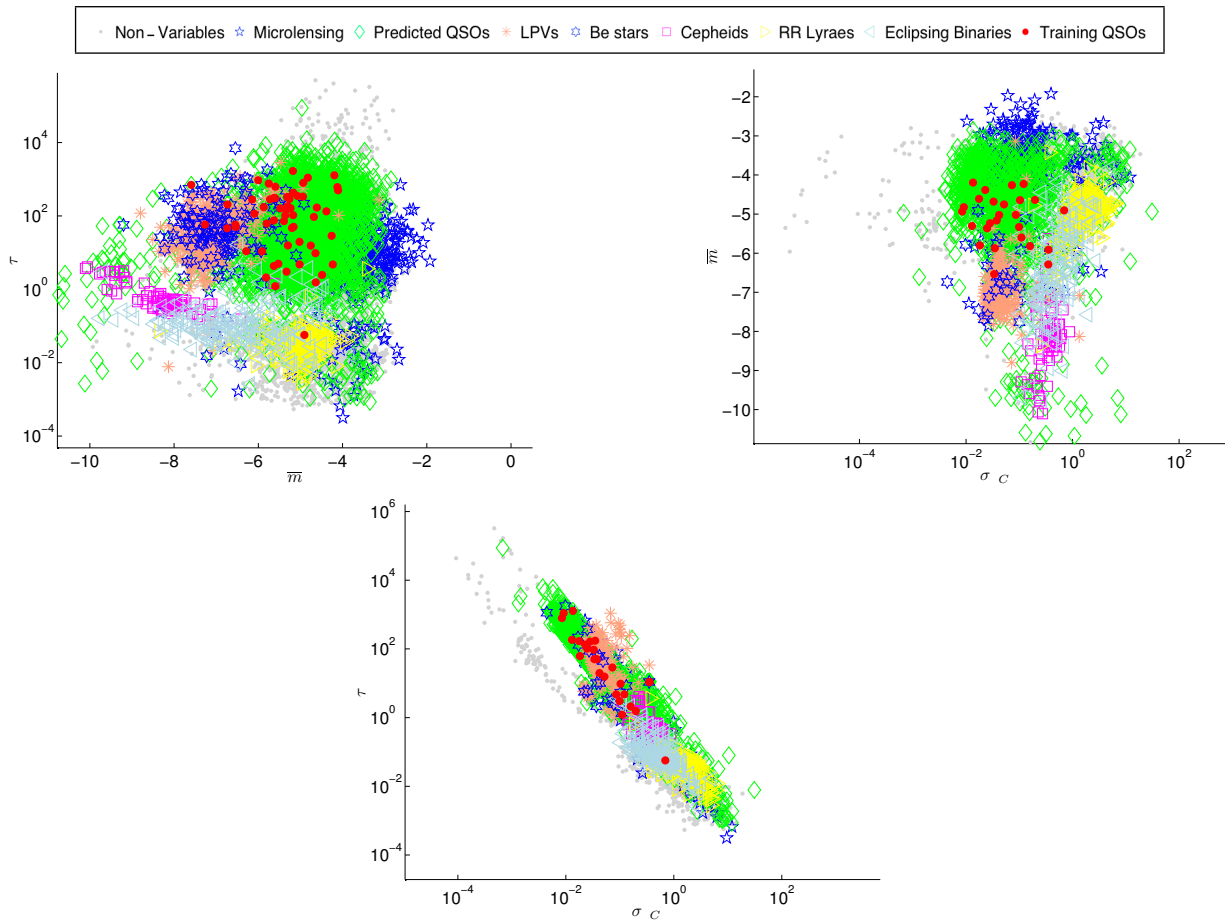


Figure 11. Predicted quasars and training stars distributions projected on different pairs of CAR(1) features for MACHO data.

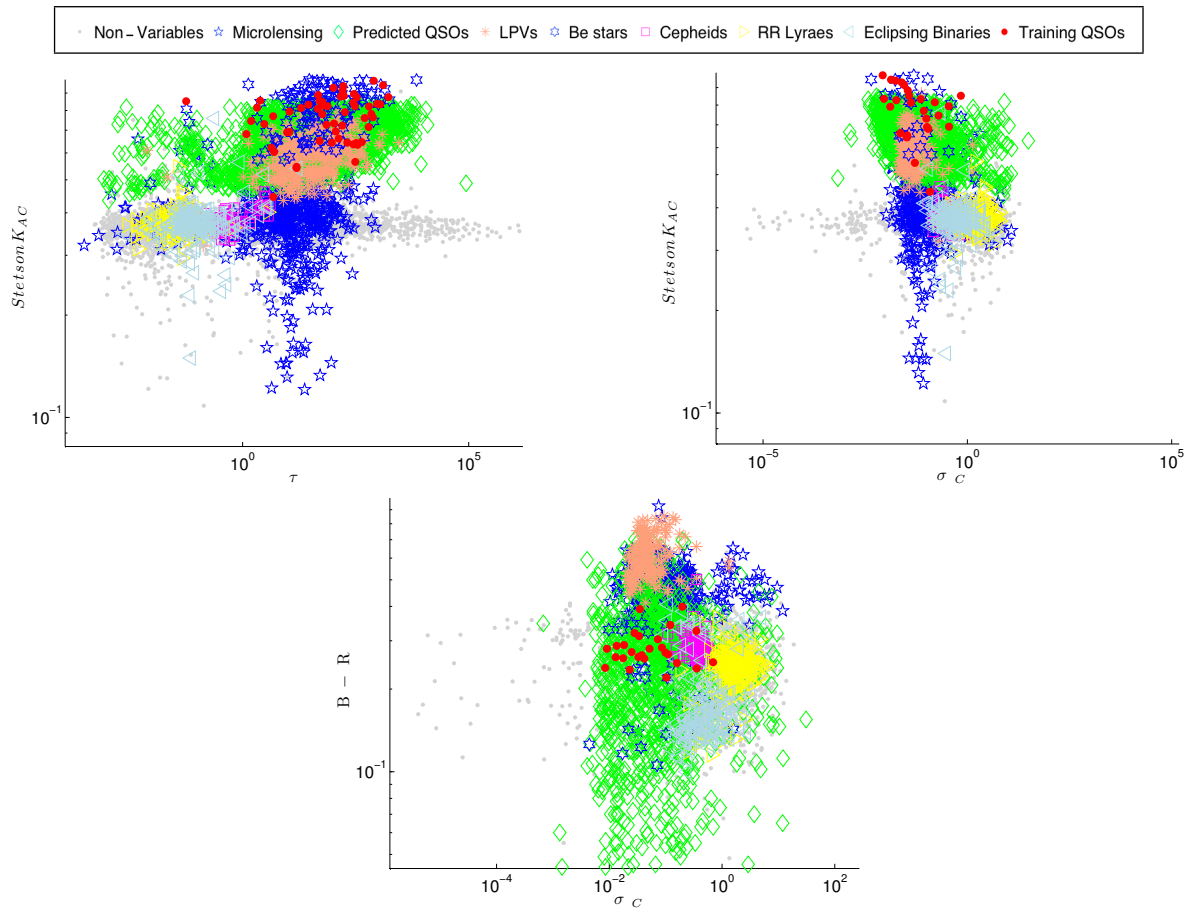


Figure 12. Predicted quasars and Training stars distributions for σ_C and τ features combined with three time series features for MACHO data.